

This work has been submitted to the IEEE for possible publication. Copyright may be transferred without notice, after which this version may no longer be accessible.

A Mixed-Integer Approach for Motion Planning of Nonholonomic Robots under Visible Light Communication Constraints

Angelo Caregnato-Neto^{1,2,*}, Marcos R. O. A. Maximo³, and Rubens J. M. Afonso¹,

¹*Electronic Engineering Division, Instituto Tecnológico de Aeronáutica, São José dos Campos, Brazil*

²*Delft University of Technology, The Netherlands.*

³*Autonomous Computational Systems Lab (LAB-SCA), Computer Science Division, Instituto Tecnológico de Aeronáutica, São José dos Campos, Brazil*

^{*}*Corresponding author (caregnato.neto@ieee.org)*

Abstract—This work addresses the problem of motion planning for a group of nonholonomic robots under Visible Light Communication (VLC) connectivity requirements. In particular, we consider an inspection task performed by a Robot Chain Control System (RCCS), where a leader must visit relevant regions of an environment while the remaining robots operate as relays, maintaining the connectivity between the leader and a base station. We leverage Mixed-Integer Linear Programming (MILP) to design a trajectory planner that can coordinate the RCCS, minimizing time and control effort while also handling the issues of directed Line-Of-Sight (LOS), connectivity over directed networks, and the nonlinearity of the robots' dynamics. The efficacy of the proposal is demonstrated with realistic simulations in the Gazebo environment using the Turtlebot3 robot platform.

Index Terms—Multi-agent systems, Line of sight communication, Directed graph connectivity, Trajectory planning, Differential robots

I. INTRODUCTION

Visible Light Communication (VLC) is a wireless transmission technology in which information is exchanged through the modulation of visible light beams [1]. It offers advantages such as insensitivity to electromagnetic interference and inherent network security [1]–[3]. However, any connections require a clear Line Of Sight (LOS) between the transmitter and receivers.

In [2], a Robot Chain Control System (RCCS) comprised of nonholonomic robots and supported by VLC communication was demonstrated. An RCCS is a multi-robot platform comprised of a base, transmission relays, and a leader. Its application alongside VLC has been proposed for the inspection and maintenance of pipelines and underground facilities [2]–[4]. In such situations, the base serves as a central commanding unit, whereas the relays connect the leader, responsible for the task, with the base. This chained communication network allows for the extension of the operational area of the leader. The LOS requirement has been addressed in environments with corners and obstacles with point-to-point connections generated by the relays of the RCCS [2]. However, the robots were manually operated, making their coordination challenging and susceptible to human error.

The problem of autonomous coordination of multi-robot systems with connectivity maintenance is relevant in applications such as formation control [5], coverage [6], and patrolling [7]. In [8] the deployment of UAVs for emergency networks in post-disaster scenarios is studied. A chained network is generated to transmit information back to a relief center. The problem of autonomous exploration of mines with connectivity maintenance

between robots and a base station is addressed in [9]. A global planner computes paths for robots and the non-Line-Of-Sight (nLOS) environment is handled by dropping nodes that incrementally build a network. In [10], a modular planning algorithm is designed to generate and maintain a chain between a base station and objectives in dynamic and unpredictable environments.

Alternatively, Mixed-Integer Programming (MIP) offers an optimization framework that has been successful in handling decision and motion planning problems for multi-agent systems [11]–[14]. This technique can jointly address the key issues of LOS-connectivity [13], [15], collision avoidance [16], and task allocation [11], [12]. In particular, Mixed-Integer Linear Programming (MILP) can address such complex problems in finite run-times and the use of branch-and-bound algorithms can significantly improve solver performance [17].

We propose a MILP-based motion planning algorithm that allows the autonomous operation of the RCCS while maintaining the connectivity of the underlying communication network under VLC requirements. Unlike previous proposals [13], this work addresses the issues of directed-LOS and connectivity of directed networks, as well as the nonlinear dynamics of nonholonomic robots. We formulate sufficient conditions for the connectivity of an RCCS and provide an encoding of them for MILP models as constraints. The functionality of the method is demonstrated with a realistic robotics simulation using Gazebo and the Turtlebot3 platform. This is the first algorithm to address the motion planning of an RCCS under a VLC-based communication network.

The paper is organized as follows. Section II provides a detailed description of the RCCS-VLC motion planning problem. In Section III we propose a MILP optimization model as a solution and discuss the novel constraints required. The simulation and corresponding results are presented in Section IV. The paper is concluded in Section V where we provide final remarks and future lines of research.

We employ the following notation. Implications involving binary variables, such as $b \implies \text{'o'}$, are equivalent to $b = 1 \implies \text{'o'}$. In-degrees and

out-degrees of a vertex ‘ v ’ are denoted by $\deg^-(v)$ and $\deg^+(v)$, respectively. Sets are represented by calligraphic letters as in \mathcal{M} . Sets of integers in the interval $[n_0, n_f]$ are written as $\mathcal{I}_{n_0}^{n_f}$. A vector of size n with all entries equal to one is denoted by $\mathbf{1}_n$. The Pontryagin difference operator is written as \sim [18].

II. PROBLEM DESCRIPTION

We consider an inspection problem using a wheeled RCCS similar to the one proposed in [2]. The group is comprised of $n_a \in \mathbb{N}$ nonholonomic robots with discrete-time dynamics described by, $\forall i \in \mathcal{I}_1^{n_a}$,

$$r_{x,i}(k+1) = r_{x,i}(k) + \sigma_i(k) \cos(\psi_i(k)), \quad (1)$$

$$r_{y,i}(k+1) = r_{y,i}(k) + \sigma_i(k) \sin(\psi_i(k)), \quad (2)$$

$$\sigma_i(k) = \xi_i(k)T + a_i(k)\frac{T^2}{2}, \quad (3)$$

$$\xi_i(k+1) = \xi_i(k) + a_i(k)T, \quad (4)$$

$$\psi_i(k+1) = \psi_i(k) + \Delta\psi_i(k), \quad (5)$$

where $r_{x,i} \in \mathbb{R}$ and $r_{y,i} \in \mathbb{R}$ represent the position of the i -th robot w.r.t. x and y axes of a global coordinate system, respectively; $\psi_i \in \mathbb{R}$ corresponds to the orientation of the robot w.r.t to the same coordinate system; $\sigma_i \in \mathbb{R}$, $\xi_i \in \mathbb{R}$, and $a_i \in \mathbb{R}$ are the robot’s linear displacement, velocity, and acceleration, respectively. The dynamics were discretized with a sampling period $T > 0$.

The components of the RCCS are divided into a static base and two types of mobile agents: the relays and a leader. The purpose of the latter is to perform the inspection of a region while the relays coordinate to keep the group connected to the base. See Fig. 1 for an example. For the sake of simplicity, the agents with indices 1 and n_a are always assigned as the base and the leader, respectively. The inspection finishes after all $n_t \in \mathbb{N}$ targets, representing regions of interest in the environment, are reached by the leader. The targets are written as the polytopes $\mathcal{T}_e \subset \mathbb{R}^2$, $\forall e \in \mathcal{I}_1^{n_t}$.

The base is responsible for broadcasting high-level commands, such as trajectories to be followed and targets to be visited, or emergency stop commands. The mobile agents operate in a region $\mathcal{A} \subset \mathbb{R}^2$ which contains $n_o \in \mathbb{N}$ obstacles \mathcal{O}_c , $\forall c \in \mathcal{I}_1^{n_o}$.

The space occupied by the structure of the j -th robot is represented by the polytope $\mathcal{R}_j(k), \forall j \in \mathcal{I}_1^{n_a}$, which is centered at $\mathbf{r}_j(k) = [r_{x,j}, r_{y,j}]^\top$. The allowed operation space of robot i at time step k is written as, $i \in \mathcal{I}_1^{n_a}$,

$$\bar{\mathcal{A}}_i(k) = \left\{ \mathcal{A} \setminus \left(\bigcup_{c=1}^{n_o} \mathcal{O}_c \cup \bigcup_{\substack{j=1 \\ j \neq i}}^{n_a} \mathcal{R}_j(k) \right) \right\} \sim \mathcal{R}_i. \quad (6)$$

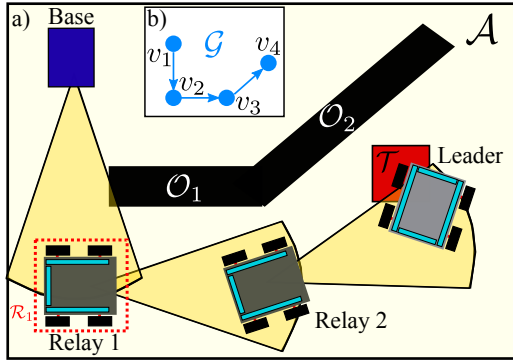


Fig. 1. Illustration of RCCS as devised in [2]. a) A base station with two relay robots and a leader connected under VLC communication. b) Corresponding chained communication network.

The system operates under a VLC-based communication network, as illustrated in Fig. 1. The relay robots are equipped with solar panel receivers attached to their sides and back, whereas the leader also has a panel attached to its front. The transmitters of the relays and base are LED spotlights. The resulting communication system is simplex, i.e. the communication occurs in a single direction, and the ensuing network can be represented by the time-indexed digraph $\mathcal{G}(k) = \{\mathcal{V}, \mathcal{E}(k)\}$, where $\mathcal{V} = \{v_1, v_2, \dots, v_{n_a}\}$ is the set of vertices, with v_1 and v_{n_a} representing the base and the leader, respectively, whereas the remaining vertices represent the relays. The set of edges is denoted by $\mathcal{E}(k)$ with edges corresponding to the time-varying connections between robots. In this context, Problem 1 specifies the issues to be addressed henceforth.

Problem 1. *Develop an algorithm to plan trajectories for the RCCS such that:*

- a) *physical constraints of the robots are respected;*
- b) *the base remains connected with the leader;*
- c) *the robots avoid collisions;*
- d) *a compromise between time and control effort is minimized;*
- e) *all targets are visited by the leader.*

III. MILP MOTION PLANNING

We propose the use of MILP to solve Problem 1. This technique has been shown to effectively handle motion planning of nonholonomic robots under connectivity constraints in obstacle-filled scenarios [19]. However, linear models were employed in the motion planning module with the resulting mismatches being handled by tracking controllers. Consequently, the proposed scheme was unable to explicitly consider the robot's orientation as a decision variable. Since the connectivity of the RCCS relies on the full pose of each robot, the nonlinear dynamics represented by (1) and (2) must be integrated into the model, allowing the constrained optimization of ψ . Additionally, the requirements of directed-LOS for connections and the connectivity maintenance of the ensuing network also represent novel challenges. The solutions for these problems are now presented.

A. Dynamics constraints

To accommodate the nonlinear dynamics of (1) and (2) in the MILP model, we start by assuming that the orientation is constrained to a discrete set of $n_{ori} \in \mathbb{N}$ possible values $\mathcal{S}_i = \{\hat{\psi}_{i,g}\}$, $i \in \mathcal{I}_1^{n_a}$, $\forall g \in \mathcal{I}_1^{n_{ori}}$, with

$$\hat{\psi}_{i,g} = \frac{2\pi(g-1)}{n_{ori}}. \quad (7)$$

Considering a maximum horizon of $\bar{N} \in \mathbb{N}$ time steps, the dynamics are now encoded as lin-

ear constraints with binary variables, $\forall i \in \mathcal{I}_1^{n_a}$, $\forall g \in \mathcal{I}_1^{n_{ori}}$, $\forall k \in \mathcal{I}_0^{\bar{N}}$,

$$\begin{aligned} r_{x,i}(k+1) &\leq r_{x,i}(k) + \\ &\quad \sigma_i(k) \cos(\hat{\psi}_{i,g}(k)) + (1 - b_{i,g}^{ori}(k))M, \end{aligned} \quad (8)$$

$$\begin{aligned} -r_{x,i}(k+1) &\leq -r_{x,i}(k) - \\ &\quad \sigma_i(k) \cos(\hat{\psi}_{i,g}(k)) + (1 - b_{i,g}^{ori}(k))M, \end{aligned} \quad (9)$$

$$\begin{aligned} r_{y,i}(k+1) &\leq r_{y,i}(k) + \\ &\quad \sigma_i(k) \sin(\hat{\psi}_{i,g}(k)) + (1 - b_{i,g}^{ori}(k))M, \end{aligned} \quad (10)$$

$$\begin{aligned} -r_{y,i}(k+1) &\leq -r_{y,i}(k) - \\ &\quad \sigma_i(k) \sin(\hat{\psi}_{i,g}(k)) + (1 - b_{i,g}^{ori}(k))M, \end{aligned} \quad (11)$$

where $b_{i,g}^{ori} \in \{0, 1\}^{n_{ori}}$ is the orientation binary variable and $M \in \mathbb{R}$ is the ‘‘Big-M’’ constant [20]. Through constraints (8)-(11) the dynamics are written for every possible orientation in \mathcal{S}_i . Naturally, each robot is oriented towards one particular angle at each time step and the aforementioned constraints must be imposed only for this orientation. Thus, the following constraint is imposed, $\forall i \in \mathcal{I}_1^{n_a}$, $\forall k \in \mathcal{I}_0^{\bar{N}}$

$$\sum_{g=1}^{n_{ori}} b_{i,g}^{ori}(k) = 1. \quad (12)$$

Constraint (12) guarantees that (8)-(11) are only active for one orientation at each time step, while the remaining constraints are relaxed by the ‘‘Big-M constant’’. The actual angle at time step k is written as $\psi_i(k) = \Psi^\top \mathbf{b}_i^{ori}(k)$ where

$$\Psi = [\hat{\psi}_{i,1}, \hat{\psi}_{i,2}, \dots, \hat{\psi}_{i,n_{ori}}]^\top, \quad (13)$$

$$\mathbf{b}_i^{ori}(k) = [b_{i,1}^{ori}(k), b_{i,2}^{ori}(k), \dots, b_{i,n_{ori}}^{ori}(k)]^\top. \quad (14)$$

This approach allows the trigonometric functions in (8)-(11) to be computed beforehand for each possible orientation, yielding linear constraints suitable for the MILP model. The remaining dynamics (3), (4), and (5) are written directly as linear constraints.

B. Network connectivity

The purpose of the cation network in an RCCS is to transmit commands from the base station to the leader. Therefore, RCCS connectivity is defined as follows.

Definition 1. An RCCS is connected at time step k if its communication graph $\mathcal{G}(k)$ contains a directed path between the vertices v_1 and v_{n_a} .

We propose constraints for the MILP model that guarantee RCCS connectivity at each time step. The first step is to encode the vertices’ in-degrees and out-degrees respectively as, $\forall i \in \mathcal{I}_1^{n_a}$, $\forall k \in \mathcal{I}_0^{\bar{N}}$,

$$\deg_i^-(k) = \sum_{\substack{j \in \mathcal{I}_1^{n_a} \\ j \neq i}} b_{j,i}^{con}(k), \quad (15)$$

$$\deg_i^+(k) = \sum_{\substack{j \in \mathcal{I}_1^{n_a} \\ j \neq i}} b_{i,j}^{con}(k), \quad (16)$$

where $b_{i,j}^{con} \in \{0, 1\}$ is the connectivity binary. The activation of $b_{i,j}^{con}$ implies the existence of a directed edge from vertex i towards vertex j and the corresponding conditions for activation will be discussed in Section III-C. The following constraints are now proposed for RCCS connectivity, $\forall k \in \mathcal{I}_0^{\bar{N}}$,

$$\deg_1^-(k) = 0, \quad (17)$$

$$\deg_{n_a}^+(k) = 0, \quad (18)$$

$$\deg_m^-(k) = 1, \quad \forall m \in \mathcal{I}_2^{n_a}, \quad (19)$$

$$\deg_m^+(k) = 1, \quad \forall m \in \mathcal{I}_1^{n_a-1}. \quad (20)$$

Theorem 1. Satisfaction of constraints (17)-(20) guarantees that the RCCS is connected.

Proof. Constraints (17) and (20) enforce that v_1 must be connected towards some vertex $v' \in \mathcal{V} \setminus \{v_1\}$. Either, $v' = v_{n_a}$ and there is a directed path between base and leader, or $v' = v_i$, $i \in \mathcal{I}_2^{n_a-1}$, represents a relay. In the second case, in view of (20), v' must be connected towards some other vertex $v'' \in \mathcal{V} \setminus \{v_1, v'\}$. Again, either $v'' = v_{n_a}$ and the network is connected, or $v'' \neq v_{n_a}$. In the latter case, v'' must connect to another a vertex $v''' \in \mathcal{V} \setminus \{v_1, v', v''\}$ in light of (20) and so on. Since the number of vertices n_a is finite, this process can be repeated at most $n_a - 1$ times

before reaching v_{n_a} . Constraint (19) imposes that any subsequent relay connections that are formed due to (20) add a distinct vertex to the chained digraph. Since there is a finite number of relays, this chain is also finite and eventually must reach a sink. Constraint (18) allows only v_{n_a} to be a sink. Thus, the chain must contain v_{n_a} and there is a directed path between the vertices representing the base and the leader. It follows that the RCCS is connected according to Definition 1. \square

C. Directed conic LOS

The first condition for VLC-based connections is that there must be a clear LOS between the robots. The LOS between robots i and j is considered clear at time step k if there are no obstacles obstructing it [13], i.e., $i \in \mathcal{I}_1^{n_a}$, $j \in \mathcal{I}_1^{n_a} \setminus i$, $\forall c \in \mathcal{I}_1^{n_o}$,

$$\mathcal{L}_{i,j}(k) \cap \mathcal{O}_c = \emptyset, \quad (21)$$

where $\mathcal{L}_{i,j} = \{\mathbf{p} \in \mathbb{R}^2 \mid \mathbf{p} = \mathbf{r}_i \alpha + \mathbf{r}_j (1 - \alpha), \forall \alpha \in [0, 1]\}$ with $\mathbf{r}_i = [r_{x,i}, r_{y,i}]^\top$ and $\mathbf{r}_j = [r_{x,j}, r_{y,j}]^\top$, i.e., $\mathcal{L}_{i,j}$ is the line segment connecting the position of the two robots. Condition (21) is enforced by the following constraint, $i \in \mathcal{I}_1^{n_a}$, $j \in \mathcal{I}_1^{n_a} \setminus i$, $\forall c \in \mathcal{I}_1^{n_o}$, $\forall k \in \mathcal{I}_0^N$,

$$b_{i,j}^{con}(k) \implies \mathcal{L}_{i,j}(k) \cap \mathcal{O}_c = \emptyset. \quad (22)$$

For details on the implementation of (22), see [13].

The second condition is that the receiver must be within the cone of light generated by the transmitter. The LED spotlights of the robots are rigidly attached to their body, so the cone shares the same orientation as the robot. The cone is parametrized by its aperture θ and range h as illustrated in Fig. 2. For the sake of simplicity, its apex is positioned at the geometric center of the robot, but the method allows for different positioning depending on where the spotlights are installed. We approximate the cones for each possible orientation as polytopes with the following halfspace representation, $\forall i \in \mathcal{I}_1^{n_a}$, $\forall g \in \mathcal{I}_1^{n_{ori}}$,

$$\mathcal{C}_{i,g} = \{\mathbf{z} \in \mathbb{R}^2 \mid \mathbf{P}_{i,g} \mathbf{z} \leq \mathbf{q}_{i,g}\}, \quad (23)$$

with $\mathbf{P}_{i,g} \in \mathbb{R}^{n_s \times 2}$ and $\mathbf{q}_{i,g} \in \mathbb{R}^{n_s}$ where $n_s \in \mathbb{N}$ is the number of sides of the polygon $\mathcal{C}_{i,g} \subset \mathbb{R}^2$.

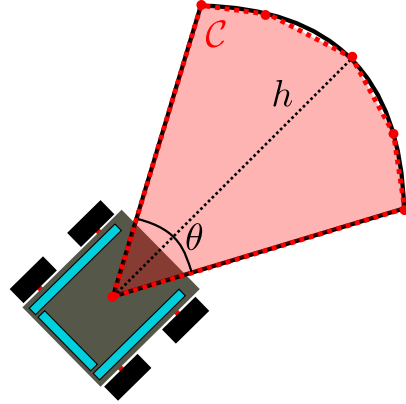


Fig. 2. Original and polytopic approximation of RCCS's conic light beams.

Define the relative position $\tilde{\mathbf{r}}_{i,j} \triangleq \mathbf{r}_j - \mathbf{r}_i$, $i \neq j$. Then, the directed conic LOS constraint can be written as, $\forall g \in \mathcal{I}_1^{n_{ori}}$, $\forall i \in \mathcal{I}_1^{n_a}$, $\forall j \in \mathcal{I}_1^{n_a} \setminus i$, $\forall k \in \mathcal{I}_0^N$

$$\mathbf{P}_{i,g} \tilde{\mathbf{r}}_{i,j}(k) \leq \mathbf{q}_{i,g} + (1 - b_{i,g}^{ori}(k))M + (1 - b_{i,j}^{con}(k))M. \quad (24)$$

Proposition 1. Let $\psi_{i,h}(k)$ be the orientation of the transmitter i at time step k . Then, $b_{i,j}^{con}(k) = 1$ and the satisfaction of (22) and (24) imply that receiver j is within the unobstructed light cone of the transmitter i .

Proof. Constraint (22) guarantees that if $b_{i,j}^{con}(k) = 1$, then there is a clear LOS between robots. See [13] for a proof. If the orientation of transmitter i is $\psi_{i,h}$ then only $b_{i,h}^{ori} = 1$ due to (12). Since $b_{i,j}^{con}(k) = 1$, the particular inequality $\mathbf{P}_{i,h} \tilde{\mathbf{r}}_{i,j}(k) \leq \mathbf{q}_{i,h}$ from (24) is not relaxed by the “Big-M” approach and consequently must hold. From these conclusions, it follows the receiver must be within an unobstructed region of the transmitter's cone of light. \square

Finally, since the relay robots are not equipped with solar panels in their front, they are not allowed to form connections while facing each other or the base. An approximation for this condition can be attained by guaranteeing that the transmitter is never within the cone of light of the receiver. Let $\mathbf{b}_{i,j,g}^{fro} =$

$[b_{1,i,j,g}^{fro}, \dots, b_{n_s,i,j,g}^{fro}]$ be a vector of $n_s \in \mathbb{N}$ binaries. Then, we propose the following constraints, $\forall g \in \mathcal{I}_1^{n_{ori}}, \forall i \in \mathcal{I}_1^{n_a-1}, \forall j \in \mathcal{I}_1^{n_a-1} \setminus i, \forall k \in \mathcal{I}_0^N$

$$-\mathbf{P}_{j,g} \tilde{\mathbf{r}}_{j,i}(k) \leq -\mathbf{q}_{j,g} + (\mathbf{1}_{n_s} - \mathbf{b}_{i,j,g}^{fro}(k))M, \quad (25)$$

$$b_{i,j}^{con}(k) \leq \sum_{z=1}^{n_s} b_{z,i,j,g}^{fro}(k) + (1 - b_{j,g}^{ori}(k)). \quad (26)$$

Constraint (25) is similar to the obstacle avoidance constraints in [12]. It guarantees that the i -th robot is not within the cone of light of the j -th robot if at least one entry of $\mathbf{b}_{i,j,h}^{fro}$ takes the value of 1. Constraint (26) conditions the activation of $b_{i,j}^{con}$ to at least one entry $\mathbf{b}_{i,j,g}^{fro}$ taking the value of 1. The orientation binary guarantees that this constraint is only enforced for the cone with appropriate orientation.

D. Rotation dynamics compensation

In the proposed motion planning algorithm the assumption that the robots can reach the commanded orientations instantly is made, as shown in (5). To adhere to this assumption, we compensate for the rotation dynamics delay through the manipulation of the cone polytope.

Let Δt denote the maximum time taken by a robot to rotate a maximum orientation increment of $\pm \Delta \psi^{max}$. To compensate for the delay in rotation, one must ensure that the receiver robot is still within the light cone of the transmitter after moving for Δt s. The maximum displacement of a robot during this time is $d = \xi^{max} \Delta t$, where $\xi^{max} > 0$ is the maximum linear velocity of the robots. Thus, we compensate for the potential movement of the receiver by planning the trajectories considering light cone polytopes $\mathcal{C}_{i,g}$ contracted by d in all directions. This is accomplished with the following operation, $\forall i \in \mathcal{I}_1^{n_a}, \forall g \in \mathcal{I}_1^{n_{ori}}$,

$$\bar{\mathcal{C}}_{i,g} = \mathcal{C}_{i,g} \sim \mathcal{B}_d, \quad (27)$$

where $\bar{\mathcal{C}}_{i,g} \subset \mathbb{R}^2$ is a contracted cone and $\mathcal{B}_d \subset \mathbb{R}^2$ a ball of radius d and centered at the origin.

In order to enforce the orientation increment to be bounded, we start by addressing the issue

of discontinuities in the trigonometric functions. This is accomplished with the following constraints, $\forall i \in \mathcal{I}_1^{n_a}, \forall k \in \mathcal{I}_0^N$,

$$\Delta \psi_i(k) \leq \pi + b_{i,1}^{disc}(k)M, \quad (28)$$

$$-\Delta \psi_i(k) \leq \pi + b_{i,2}^{disc}(k)M, \quad (29)$$

$$\Delta \bar{\psi}_i(k) = \Delta \psi_i(k) - 2\pi(1 - b_{i,1}^{disc}(k)) + 2\pi(1 - b_{i,2}^{disc}(k)). \quad (30)$$

Constraints (28) and (29) enforce that if $\Delta \psi_i$ lie outside the desired interval of $[-\pi, \pi]$ due to the discontinuities, then one of the binary variables $b_{i,1}^{disc} \in \{0, 1\}$ or $b_{i,2}^{disc} \in \{0, 1\}$ are activated, whereas (30) updates a new variable $\Delta \bar{\psi}_i(k)$ with the appropriate correction by summing or subtracting 2π . Now, the orientation increment bounds are enforced to be within the interval $[\Delta \psi_i^{min}, \Delta \psi_i^{max}]$ by the constraints, $\forall i \in \mathcal{I}_1^{n_a}, \forall k \in \mathcal{I}_0^N$,

$$\Delta \bar{\psi}_i(k) \leq \Delta \psi_i^{max}, \quad (31)$$

$$-\Delta \bar{\psi}_i(k) \leq \Delta \psi_i^{min}. \quad (32)$$

E. Optimization problem

Let $\boldsymbol{\lambda} = [\mathbf{r}_i, \xi_i, a_i, N, b_e^{tar}, b_{i,j}^{con}, b_{i,j}^{ori}, b_{i,1}^{disc}, b_{i,2}^{disc}]$ denote the vector of all optimization variables. Then the motion planning optimization is written as the following.

Motion planning problem.

$$\min_{\boldsymbol{\lambda}} N + \sum_{k=0}^N \sum_{i=1}^{n_a} (\gamma_a \|\mathbf{a}_i(k)\|_1 + \gamma_{\Delta \psi} \|\Delta \psi_i(k)\|_1) \quad (33a)$$

$$\text{s.t., } \forall i \in \mathcal{I}_1^{n_a}, \forall c \in \mathcal{I}_1^{n_o}, \forall e \in \mathcal{I}_1^{n_t}, \forall k \in \mathcal{I}_0^N,$$

$$(3), (4), (8-12), (15-20), (22), (24-26) (28-32)$$

$$\xi_i^{min} \leq \xi_i(k) \leq \xi_i^{max}, \quad (33b)$$

$$a_i^{min} \leq a_i(k) \leq a_i^{max}, \quad (33c)$$

$$\mathbf{r}_i(k+1) \in \bar{\mathcal{A}}_i(k+1), \quad (33d)$$

$$b_e^{tar}(k) \implies \mathbf{r}_{n_a}(k) \in \mathcal{T}_e, \quad (33e)$$

$$\sum_{k=0}^N b_e^{tar}(k) = 1. \quad (33f)$$

The cost (33a) is a compromise between time expenditure, represented by the variable horizon

$N \in \mathbb{N}$ [21], the acceleration effort weighted by $\gamma_a > 0$, and the orientation increments weighted by $\gamma_{\Delta\psi} > 0$. Constraints (33b) and (33c) enforce the linear velocities and accelerations to be within the bounds determined by their corresponding minimum and maximum excursions, $[\xi^{min}, \xi^{max}]$ and $[a^{min}, a^{max}]$, respectively. Collision avoidance is guaranteed by constraint (33d). Finally, (33e) and (33f) enforce that all targets are visited by the leader within the maximum horizon \bar{N} . The implementation of (33a)-(33e) is omitted for the sake of brevity. The reader is referred to [12] and [13] for a thorough presentation. We also provide the code for the motion planning algorithm as open source¹.

IV. RESULTS

We evaluate our algorithm through a simulation of the Turtlebot3 robot platform in the Gazebo environment. The orientation control law was designed as a proportional controller with gain $K_p = 6.5$, whereas the linear velocity uses only a feedforward controller. After experiments with the proposed control laws considering the robot's maximum linear velocity to be $\xi^{max} = 0.22$ m/s, we concluded that in the worst case scenario $\Delta t \approx 1$ s considering orientation increment bounds of $\Delta\psi^{min} = -60^\circ$ and $\Delta\psi^{max} = 60^\circ$ resulting in $d \approx 0.22$ m. Safety margins of $\epsilon = 0.08$ m were added to all polytopes to handle potential disturbances and tracking errors.

The bodies of the robots were approximated by the square that circumscribes the circle with a diameter equal to the length of the robot, 0.178 m. The parameters of the light cone were selected as $\theta = 60^\circ$, $h = 2.8$ m. The base is introduced in the problem using the same constraints but considering a static agent. Since the Turtlebot3 operates with relatively low velocities, we employed a sampling period $T = 4$ s and a maximum horizon $\bar{N} = 9$. The total number of orientations was chosen as $n_\psi = 12$, corresponding to steps of 30° . The light cone was approximated by a polytope with $n_s = 6$ sides. The optimization weights were selected as $\gamma_a = 0.1$ and $\gamma_{\Delta\psi} = 0.1$.

¹https://gitlab.com/caregnato_neto_open/MILP_VLC_motion_planning

The planning problem was solved in a notebook equipped with an Intel® i5-1135G7 (2.40 GHz clock) CPU and 16 GB of RAM using the Gurobi solver [22]. The optimization model was built using the Yalmip [23] and MPT toolboxes [24]. We established a limit computation time of 360 s resulting in a feasible solution with an optimality gap of 4.2%.

Fig. 3a shows the commanded and followed trajectories of the RCCS in an environment with width and length of 4 m and 3 m, respectively, as well as two targets and obstacles. The group was able to track the trajectories, demonstrating that the algorithm was able to compute adequate motion considering the physical limitations of the robots. The maximum tracking error was 0.078 m, which is within the expected margins. The optimal horizon was $N = 8$, corresponding to the mission being finished after 28 seconds; after this period, the group is commanded to stop translation. Fig 3b depicts the terminal pose of the RCCS.

The snapshots of the maneuver at each instant $kT + \Delta t$ and the corresponding light beams of the base and robots are presented in Fig. 4. Using the planned trajectories the relays were able to successfully coordinate, maintaining the connectivity of the network at the appropriated time steps while the leader reached both targets. No collisions occurred. The commanded orientation increments were always kept within the desired bounds, as illustrated by Fig. 5, allowing each robot to reach the desired orientation within the required time interval.

V. CONCLUSION

This work addressed the motion planning problem of an RCCS under VLC connectivity constraints. The proposed MILP-based formulation was able to compute a high-quality solution in terms of trajectories for the group of robots, resulting in appropriate coordination. The functionality was demonstrated using realistic Gazebo simulations where a group of Turtlebots completed a mission while maintaining connectivity and avoiding collisions. Future formulations can integrate the decision problem of switching the size of the luminosity

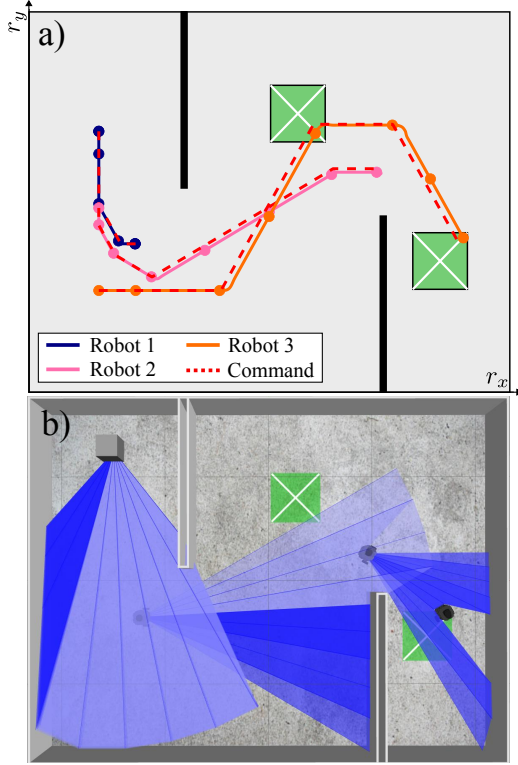


Fig. 3. a) Trajectories computed by the MILP algorithm and tracking performance of the Turtlebots3 during the Gazebo simulation depicted in b) Final pose of the robots in the simulator. Simulation video available at: <https://www.youtube.com/watch?v=xDju9YRVrtg>

cones to preserve battery life. Alternative connectivity conditions can also be studied to allow a flexible network topology. Experiments with real robots would further validate the proposal.

ACKNOWLEDGMENTS

This study was financed in part by the Coordenação de Aperfeiçoamento de Pessoal de Nível Superior - Brasil (CAPES) - Finance Code 001. Marcos Maximo is partially funded by CNPq - National Research Council of Brazil through the grant 307525/2022-8.

REFERENCES

- [1] F. A. B. Merdan, S. P. Thiagarajah, and K. Dambul, "Non-line of sight visible light communications: A technical and application based survey," *Optik*, vol. 259, p. 168982, 2022.
- [2] W. Zhao, M. Kamezaki, K. Yamaguchi, M. Konno, A. Onuki, and S. Sugano, "A wheeled robot chain control system for underground facilities inspection using visible light communication and solar panel receivers," *IEEE/ASME Trans. Mechatron*, vol. 27, no. 1, pp. 180–189, 2022.
- [3] W. Zhao, M. Kamezaki, K. Yoshida, K. Yamaguchi, M. Konno, A. Onuki, and S. Sugano, "A preliminary experimental study on control technology of pipeline robots based on visible light communication," in *2019 IEEE/SICE Int. Symp. on Sys. Integration (SII)*, 2019, pp. 22–27.
- [4] —, "A coordinated wheeled gas pipeline robot chain system based on visible light relay communication and illuminance assessment," *Sensors*, vol. 19, no. 10, 2019.
- [5] J. Zhao, K. Zhu, H. Hu, X. Yu, X. Li, and H. Wang, "Formation control of networked mobile robots with unknown reference orientation," *IEEE/ASME Trans. Mechatron*, pp. 1–13, 2023.
- [6] S. Wu, Z. Pu, T. Qiu, J. Yi, and T. Zhang, "Deep-reinforcement-learning-based multitarget coverage with connectivity guaranteed," *IEEE Trans. Ind. Inf.*, vol. 19, no. 1, pp. 121–132, 2023.
- [7] J. Scherer, A. P. Schoellig, and B. Rinner, "Min-max vertex cycle covers with connectivity constraints for multi-robot patrolling," *IEEE Rob. Autom. Lett.*, vol. 7, no. 4, pp. 10 152–10 159, 2022.
- [8] K. G. Panda, S. Das, D. Sen, and W. Arif, "Design and deployment of UAV-aided post-disaster emergency network," *IEEE Access*, vol. 7, pp. 102 985–102 999, 2019.
- [9] K. Otsu, S. Tepsuporn, R. Thakker, T. S. Vaquero, J. A. Edlund, W. Walsh, G. Miles, T. Heywood, M. T. Wolf, and A.-A. Agha-Mohammadi, "Supervised autonomy for communication-degraded subterranean exploration by a robot team," in *2020 IEEE Aerospace Conf.*, 2020, pp. 1–9.
- [10] Y. Marchukov and L. Montano, "Multi-robot coordination for connectivity recovery after unpredictable environment changes," *IFAC-PapersOnLine*, 2019.
- [11] J. Bellingham, A. Tillerson, Michaeland Richards, and J. P. How, "Multi-task allocation and path planning for cooperating UAVs," *Cooperative Control: Models, Applications and Algorithms*, pp. 23–41, 2003.
- [12] R. J. M. Afonso, M. R. O. A. Maximo, and R. K. H. Galvão, "Task allocation and trajectory planning for multiple agents in the presence of obstacle and connectivity constraint with mixed-integer linear programming," *Int. J. Robust Nonlinear Control*, vol. 30, no. 14, pp. 5464–5491, 2020.
- [13] A. Caregnato-Neto, M. R. Maximo, and R. J. Afonso, "A line of sight constraint based on intermediary points for connectivity maintenance of multiagent systems using mixed-integer programming," *Eur. J. Control*, p. 100671, 2022.
- [14] D. Ioan, I. Prodan, S. Olaru, F. Stoican, and S. Niculescu, "Mixed-integer programming in motion planning," *Annu. Rev. Control*, 11 2020.

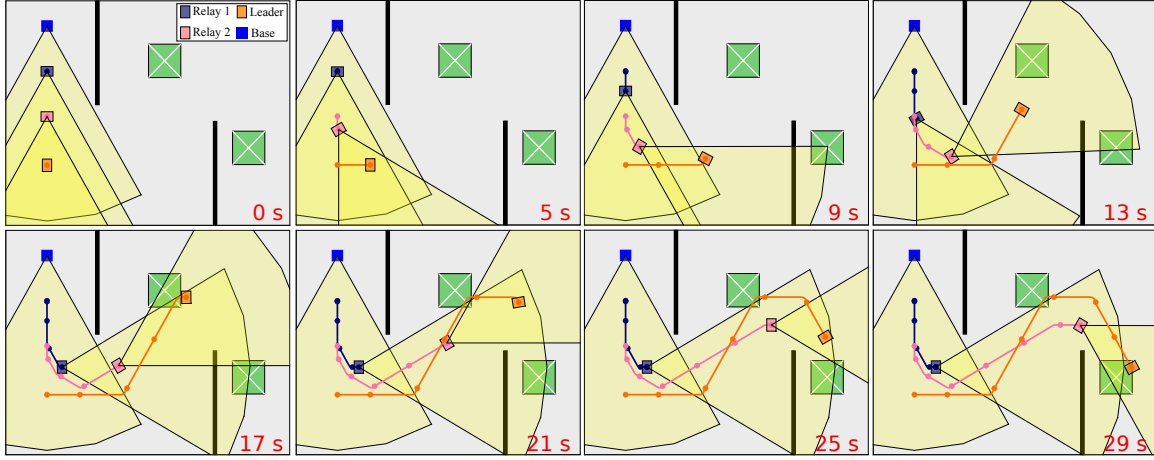


Fig. 4. Snapshots of the Turtlebots' position during Gazebo simulation at critical time steps. Green and black polygons are targets and obstacles, respectively.

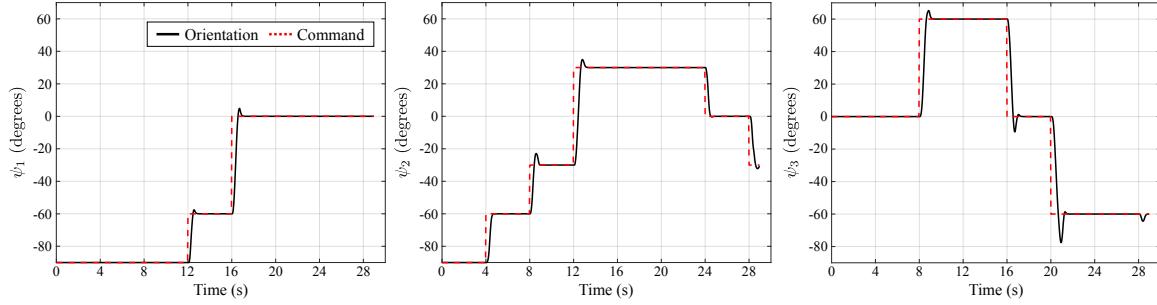


Fig. 5. Orientation of each robot during the maneuver and corresponding commands.

- [15] T. Schouwenaars, E. Feron, and J. How, "Multi-vehicle path planning for non-line of sight communication," in *Proc. of the 2006 American Control Conf.*, Minneapolis, USA., 2006.
- [16] T. Schouwenaars, B. De Moor, E. Feron, and J. How, "Mixed integer programming for multi-vehicle path-planning," in *Proc. of the 2001 European Control Conf.*, Porto, Portugal., 2001., pp. 2603–2608.
- [17] D. R. Morrison, S. H. Jacobson, J. J. Sauppe, and E. C. Sewell, "Branch-and-bound algorithms: A survey of recent advances in searching, branching, and pruning," *Discrete Optim.*, vol. 19, pp. 79–102, 2016.
- [18] M. Baotic, "Polytopic computations in constrained optimal control," *Automatika*, vol. 50, pp. 119–134, 04 2009.
- [19] A. Caregnato-Neto, M. R. O. A. Maximo, and R. J. M. Afonso, "Real-time motion planning and decision-making for a group of differential drive robots under connectivity constraints using robust MPC and mixed-integer programming," *Adv. Rob.*, vol. 37, no. 5, pp. 356–379, 2023.
- [20] A. Agarwal, S. Bhat, A. Gray, and I. E. Grossmann, "Automating mathematical program transformations," in *Practical Aspects of Declarative Languages*, M. Carro and R. Peña, Eds., Berlin, Germany, 2010, pp. 134–148.
- [21] A. Richards and J. How, "Aircraft trajectory planning with collision avoidance using mixed integer linear programming," in *Proc. of the 2002 American Control Conf.*, vol. 3, 2002, pp. 1936–1941 vol.3.
- [22] L. Gurobi Optimization, "Gurobi optimizer reference manual. <http://www.gurobi.com>," 2021.
- [23] J. Löfberg, "Yalmip: A toolbox for modeling and optimization in MATLAB," in *Proc. of 2004 IEEE Int. Conf. on Robotics and Automation.*, Taipei, Taiwan., 2004.
- [24] M. Kvasnica, P. Grieder, and M. Baotic, "Multi-Parametric Toolbox (MPT)." 2004. [Online]. Available: <http://control.ee.ethz.ch/~mpt/>

Angelo Caregnato-Neto is a PhD candidate at Instituto Tecnológico de Aeronáutica, Brazil. He is currently a visiting researcher at Delft University of Technology, Netherlands.

Marcos Omena de Albuquerque Maximo Marcos R. O. A. Maximo received the BSc degree in Computer Engineering (with Summa cum Laude honors) and the MSc and PhD degrees in Electronic and Computer Engineering from Aeronautics Institute of Technology (ITA), Brazil, in 2012, 2015, and 2017, respectively. Maximo is currently a Professor at ITA, where he is a member of the Autonomous Computational Systems Lab (LAB-SCA) and leads the robotics competition team ITAndroids. He is especially interested in humanoid robotics. His research interests also include mobile robotics, dynamical systems control, and artificial intelligence.

Rubens Junqueira Magalhães Afonso Rubens Junqueira Magalhães Afonso received his PhD (2015) and MSc (2012) degrees in Electronic and Computer Engineering and his BSc (2009) degree in Electronic Engineering from Aeronautics Institute of Technology (ITA), Brazil. During the year of 2008 he was an intern at the Institute of Aircraft Systems Engineering (IFST) at the Hamburg University of Technology (TUHH), Germany. From 2019 to 2020 he was a post-doctoral researcher at the Institute of Flight System Dynamics (FSD) in the Technical University of Munich (TUM) as a fellow from the Alexander von Humboldt Foundation. Rubens is a professor at the Systems and Control Department of the Electronic Engineering Division of ITA since 2014. His research interests include model predictive control, trajectory planning and collision avoidance, and environment exploration by autonomous agents.